Article ID: 1007-4627(2013) 03-0324-07

Effect of Isospin Dependent Cluster Recognition on Observables in Heavy Ion Collisions

ZHANG Yingxun[1], LI Zhuxia[1], ZHOU Chengshuang[1, 2], TSANG M.B.[3]

(*1. China Institute of Atomic Energy, Beijing 102413, China;*
2. College of Physics and Technology, Guangxi Normal University, Guilin 541004, Guangxi, China;
3. National Superconducting Cyclotron Laboratory, Michigan State University, East Lansing, MI 48824, USA)

Abstract: We introduce isospin dependence in the cluster recognition algorithms used in the Quantum Molecular Dynamics model to describe fragment formation in heavy ion collisions. This change reduces the yields of emitted nucleons and enhances the yields of fragments, especially for heavier fragments. The enhancement of neutron-rich lighter fragments mainly occurs at mid-rapidity. Consequently, isospin dependent observables, such as isotope distributions, yield ratios of $\frac{\mathrm{n}}{\mathrm{p}}$, $\frac{\mathrm{t}}{^3\mathrm{He}}$, $R^{\mathrm{mid}}_{\mathrm{yield}}$ and isoscaling parameters are affected. We also investigate how equilibration in heavy ion collisions is affected by this change.

Key words: isopin-dependent cluster recognition method; isospin sensitive observable; degree of system equilibrium; heavy ion collision

CLC number: O572.21; O571.6 **Document code:** A **DOI:** 10.11804/NuclPhysRev.30.03.324

1 Introduction

The productions of nucleons, light particles and intermediate mass fragments (IMF) in heavy ion collisions (HICs) provide unique experimental information about the equation of state(EoS)[1–4] as well as other equilibrium and non-equilibrium properties of nuclear matter far from its normal state[5–11]. Interpretation of the experimental results requires comparisons of data to predictions from transport models which take into account reaction dynamics. Transport models track the time evolution of a nuclear reaction, and separately treat the nuclear EoS through the mean field part and the nucleon-nucleon (NN) scattering cross sections through collision part. In detail, solving the transport models which are used to describe the heavy ion collisions require three parts: (1) Initial conditions. Such as, the reaction systems and their ground state properties, impact parameters, beam energy; (2) nucleonic potential and NN scattering cross sections which are used for simulating the nucleon propagation under nucleon-nucleon interactions; (3) cluster recognition method which is used for constructing the experimental observables through the production of fragments. The influence of the initial conditions, the mean field (both isospin dependent and independent parts) and the NN scattering cross sections has been studied by using both the Boltzmann-Uehling-Uhlenbeck (BUU) and Quantum Molecular Dynamics (QMD) approaches[12–14]. These studies also point out the importance of cluster formation in the description of reaction dynamics[2, 12–13, 15–16].

In the QMD model, fragments are formed due to A-body correlations caused by the overlapping wave packets and are identified by the cluster recognition method which also plays important roles on the final observables. At any time of the reaction process, fragments can be recognized by a minimum spanning tree (MST) algorithm[7, 17]. In this algorithm, nucleons which have a neighbor within a distance of coordinate and momentum of $|r_i - r_j| \leqslant R_0$ and $|p_i - p_j| \leqslant P_0$ belong to a fragment.

Received date: 13 Oct. 2012; **Revised date:** 10 Mar. 2013
Foundation item: National Natural Science Foundation of China (11075215, 10875031, 11005022, 11005155, 11275052); National Basic Research Program of China(973 Program)(2013CB834404); Nuclear Energy Development and Research Program in China([2011]767); National Science Foundation of USA(PHY-0606007)
Biography: ZHANG Yingxun(1976–), male, Pucheng, Shaanxi, China, Professor, working on the field of theoretical nuclear physics; E-mail: zhyx@ciae.ac.cn.

Here, the r_i and p_i are the centroids of the wavepacket for ith nucleon in their spatial and momentum space. R_0 and P_0 are phenomenological parameters determined by fitting the global experimental data, such as the intermediate mass fragments multiplicities[7, 17]. They should roughly be in the range of nucleon-nucleon interaction. Typical values of R_0 and P_0 used in the QMD approaches are about 3.5 fm and 250 MeV/c[7, 17]. This approach has been quite successful in explaining certain fragmentation observables, such as charge distributions of the emitted particles, intermediate mass fragments multiplicities[7, 17–19], yield ratios of free neutron to proton $\left(\frac{\mathrm{n}}{\mathrm{p}}\right)$, and the double $\frac{\mathrm{n}}{\mathrm{p}}$ ratios in heavy ion collisions[15]. On the other hand, the MST method fails to describe other details in the production of nucleons and light charged particles[7, 17, 20]. For example, while the yields of $Z = 1$ particles are overestimated, the yields of $Z = 2$ particles are underestimated partly due to the strong binding of α particles. Enhancements of the production of neutron-rich isotopes observed in isoscaling[21], dynamically emitted heavy fragments[22] in neutron-rich HICs, and neutron-rich light charged particles (LCP) at mid-rapidity[23] have not been described very well by simulations using transport models. Furthermore, most transport models predict more transparency than that observed experimentally in central collisions at intermediate energy[12, 24] due to insufficient production of fragments in the mid-rapidity region. Previous studies show that these problems can not be resolved by only changing the mean field or NN cross section in transport models.

There have been many attempts to improve the MST algorithm. More sophisticated algorithms such as the early cluster recognition algorithm (ECRA)[25], the simulated annealing clusterization algorithm (SACA)[26–27], and the minimum spanning tree procedure with binding energy of fragments (MSTB)[28] have been developed to provide better description of the IMF multiplicities or the average $Z_{\max}$ of the fragments. However these algorithms do not address the lack of isospin dependence in cluster recognition which is the main focus of this paper.

In the regular MST method, neutrons and protons are treated equally in the cluster recognition process, a constant maximum distance for the nucleons to be defined as belonging to a cluster is $R_0^{\mathrm{nn}} = R_0^{\mathrm{np}} = R_0^{\mathrm{pp}} = R_0 \approx 3.5$ fm. In order to investigate the effects of introducing the isospin dependence in the cluster recognition, the iso-MST, we choose different values of R_0^{nn}, R_0^{np}, and R_0^{pp}[29]. We found that $R_0^{\mathrm{nn}} = R_0^{\mathrm{np}} = 6$ fm and $R_0^{\mathrm{pp}} = 3$ fm give the largest effect on the heavy ion collisions observables in this study. These values are consistent with the R_0 values ranging from 3 to 6 fm used in the QMD simulations in order to reproduce the cluster distribution reasonably. The larger distances of R_0^{nn} and R_0^{np} take into consideration of the properties of neutron-rich nuclei, such as neutron skin or neutron halo effect, for example, a distance between halo neutron and center-of-mass for ^{11}Be is up to 7 fm. Due to the long range repulsive Coulomb force between nucleon in the cluster, a smaller R_0^{pp} value is adopted. $P_0 = 250$ MeV/c is the same in both the MST and the iso-MST methods because nucleons with large relative momentum are no longer close together in coordinate space after some time. In this paper, we compare the results calculated with the MST and the iso-MST methods to investigate effects of introducing isospin dependence in the identification of cluster formation on isospin sensitive observables. We also investigate how these cluster recognition methods affect the observable on system equilibrium. All of our studies are based on the ImQMD05 code[15, 17–19].

2 Results and discussion

Fig. 1(a) shows results of charge distributions from the central collisions of ^{124}Sn +^{124}Sn at $b = 2$ fm at 50 MeV/u beam energy calculated in the MST (open circles) and the iso-MST (solid circles), respectively. In the current paper, we adopt the convention that open circles are results obtained with the MST method, and solid circles represent results using the iso-MST method. Fig. 1(b) plots the yield ratios from the iso-MST and the MST algorithms, i.e., $\frac{Y(\text{iso-MST})}{Y(\text{MST})}$. Since larger values of R_0^{nn} and R_0^{np} are adopted, more nucleons, especially neutrons, are included in clusters. As a consequence, the multiplicities of $Z = 1$ particles are reduced by about 16%, and the production of heavier fragments with $Z > 12$ are strongly enhanced. This may explain the strong enhancement of dynamically emitted heavy fragments observed in neutron-rich heavy ion collisions[22]. Even for intermediate mass fragments with $Z = 2 \sim 12$, the multiplicities are larger by ~3%. In all cases, the enhancement is larger in neutron-rich heavy ion collisions. In order to understand the enhancement of

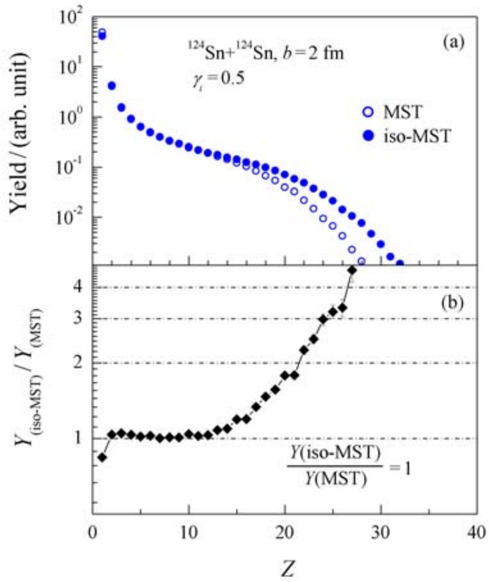

Fig. 1 (color online) (a) Charge distribution of ^{124}Sn+^{124}Sn at beam energy of $\frac{E}{A}$ = 50 MeV for b = 2 fm for $\gamma_i = 0.5$. The solid circles are results from the iso-MST algorithm and the the open circles for MST. (b) $\frac{Y(\text{iso-MST})}{Y(\text{MST})}$ ratio obtained from the same reaction system.

neutron-rich particles, we analyze the rapidity distributions of the particles emitted in central collisions of ^{124}Sn+^{124}Sn reac-tions at b = 2 fm and incident energy of E/A = 50 MeV using both the MST (open circles) and the iso-MST (solid circles) algorithms. In Fig. 2, we present the rapidity distributions of n, p, and their ratios in (a), (b) and (c), respectively. The calculations with the iso-MST method (solid circles) reduce the yields of both neutrons and protons over all rapidity regions relative to the results obtained with MST case, especially at mid-rapidity region. However, the yield ratios, $\frac{Y(\text{n})}{Y(\text{p})}$ (Fig. 2 (c)) are enhanced at mid-rapidity and become smaller at forward and backward rapidity regions in the iso-MST case than that in the MST case.

In Fig. 2 (d), (e) and (f), we plot the rapidity distributions of t, ^{3}He and their ratios, $\frac{Y(\text{t})}{Y(^3\text{He})}$, respectively. The t and ^{3}He yields are much lower than that of n and p. Note that the scales of the y-axis for Fig. 2 (d) and (e) are a factor of 10 smaller than those in Fig. 2(a) and (b). Unlike the neutron yields, the t yields (Fig. 2(d)) obtained with the iso-MST method are enhanced at mid-rapidity, and remain nearly the same in the projectile or target regions relative to the results obtained with MST method. On the other hand, there is very little difference in the yields of proton-rich ^{3}He (Fig. 2(e)) obtained with the iso-MST and the MST

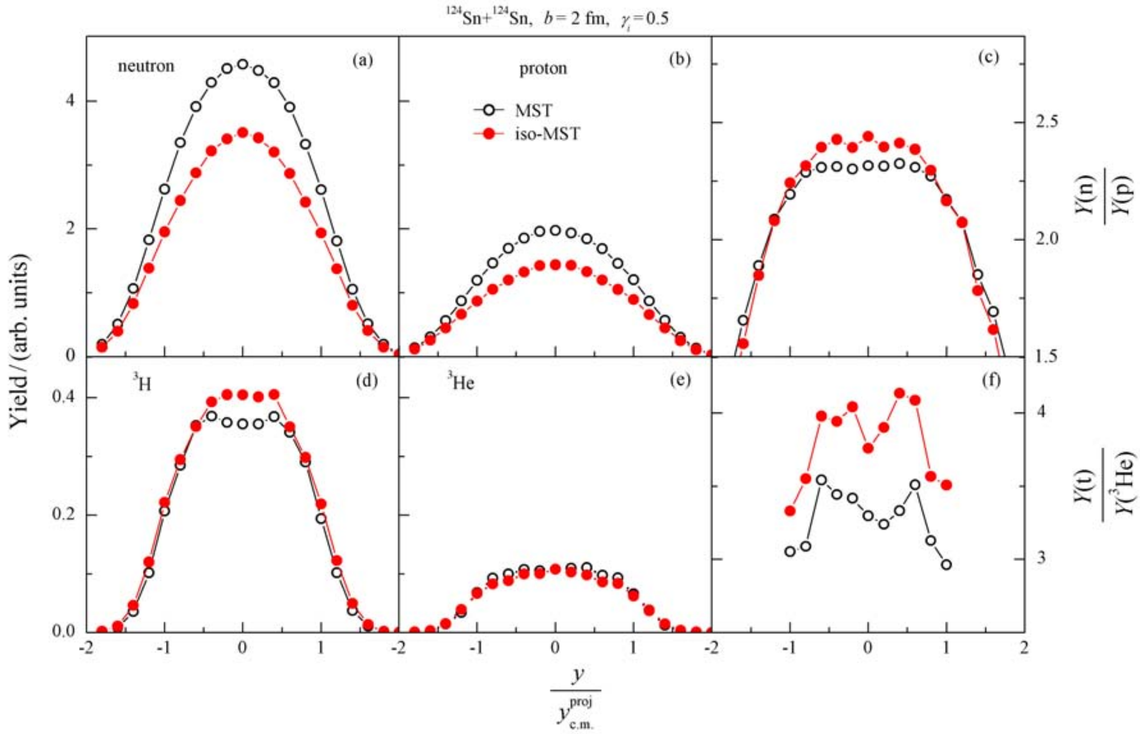

Fig. 2 (color online) The rapidity distribution of (a) the neutron yields, (b) the proton yields (c) the yield ratios, $\frac{Y(\text{n})}{Y(\text{p})}$. (d) the t yields, (e) the ^{3}He yields and (f) the yield ratios, $\frac{Y(\text{t})}{Y(^3\text{He})}$.

methods over the whole rapidity regions. As a consequence, the yields ratios, $\frac{Y(\mathrm{t})}{Y(^{3}\mathrm{He})}$, are much enhanced as shown in Fig. 2(f). The values of $\frac{Y(\mathrm{t})}{Y(^{3}\mathrm{He})}$ obtained with the iso-MST method increase to about 4.0 at mid-rapidity, much higher than the $\frac{Y(\mathrm{n})}{Y(\mathrm{p})}$ ratios. Two factors contribute to the larger $\frac{Y(\mathrm{t})}{Y(^{3}\mathrm{He})}$ ratios at mid-rapidity. First, the emitted nucleons at mid-rapidity have lower kinetic energy, because most of them pass through the expansion phase and dissipate their kinetic energy. At the end of the simulations, the emitted nucleons with lower kinetic energy are closer to the other clusters. Thus, the iso-MST algorithm with larger R_0^{nn} and R_0^{np} values will reduce the yields of nucleons at mid-rapidity as more nucleons close to the clusters are absorbed into fragments. Furthermore, production of neutron-rich fragments is enhanced at mid-rapidity due to larger $R_0^{\mathrm{nn/np}}$ values adopted in the iso-MST case. The calculated results in Fig. 2 clearly demonstrate that cluster recognition method changes the yields of nucleons and light charged particles, and neutron-rich particles emitted at mid-rapidity in heavy ion collisions.

We also analyze the influence of the iso-MST method on isospin dependent observables, such as $R\left(\frac{\mathrm{n}}{\mathrm{p}}\right)=\frac{Y(\mathrm{n})}{Y(\mathrm{p})}$, $DR\left(\frac{\mathrm{n}}{\mathrm{p}}\right)$, $DR\left(\frac{\mathrm{t}}{^{3}\mathrm{He}}\right)$ and $DR\left(\frac{t}{^{3}\mathrm{He}}\right)$ at lower and higher kinetic energy regions. In Table 1, we list the yield ratios of $\frac{\mathrm{n}}{\mathrm{p}}$ and $\frac{\mathrm{t}}{^{3}\mathrm{He}}$ with $E_{\mathrm{k}} \leqslant 40$ MeV and $E_{\mathrm{k}} \geqslant 40$ MeV for the neutron rich reaction system $^{124}\mathrm{Sn}+^{124}\mathrm{Sn}$. It is clear that the iso-MST case increases the values of $R\left(\frac{\mathrm{n}}{\mathrm{p}}\right)$ at lower kinetic energy relative to the MST case. To reduce systematic uncertainties in experiments, we also construct the double ratios $DR\left(\frac{\mathrm{n}}{\mathrm{p}}\right)$ obtained from two reaction systems $^{124}\mathrm{Sn}+^{124}\mathrm{Sn}$, $^{112}\mathrm{Sn}+^{112}\mathrm{Sn}$ at $b=2$ fm using both the iso-MST and the MST algorithms. Here

$$DR\left(\frac{\mathrm{n}}{\mathrm{p}}\right)=\frac{\left[\frac{Y(\mathrm{n})}{Y(\mathrm{p})}\right]_{^{124}\mathrm{Sn}+^{124}\mathrm{Sn}}}{\left[\frac{Y(\mathrm{n})}{Y(\mathrm{p})}\right]_{^{112}\mathrm{Sn}+^{112}\mathrm{Sn}}}\ . \qquad (1)$$

For nucleons with low kinetic energy (< 40 MeV), $DR\left(\frac{\mathrm{n}}{\mathrm{p}}\right)$ obtained in the iso-MST case is larger by about 8.3%. For nucleons with high kinetic energy (> 40 MeV), the difference between the $DR\left(\frac{\mathrm{n}}{\mathrm{p}}\right)$ values obtained from both the MST and the iso-MST cases is much less. As most of the emitted triton and ^{3}He have kinetic energies less than 40 MeV per nucleon, we list the $R\left(\frac{\mathrm{t}}{^{3}\mathrm{He}}\right)$ and $DR\left(\frac{\mathrm{t}}{^{3}\mathrm{He}}\right)$ values with $\frac{E_{\mathrm{k}}}{A}<40$ MeV in the fifth and sixth row of Table 1. The iso-MST algorithm enhances the $R\left(\frac{\mathrm{t}}{^{3}\mathrm{He}}\right)$ and $DR(\frac{\mathrm{t}}{^{3}\mathrm{He}})$ values more than those of $R\left(\frac{\mathrm{n}}{\mathrm{p}}\right)$ and $DR\left(\frac{\mathrm{n}}{\mathrm{p}}\right)$. In the seventh and eighth row of Table 1, we give the values of $R_{\mathrm{yield}}^{\mathrm{mid}}(X)=\frac{2Y_X(0<y^0<0.5)}{Y_X(0.5<y^0<1.5)}$ for the reaction system $^{70}\mathrm{Zn}+^{70}\mathrm{Zn}$ at $b=4$ fm and $E_{\mathrm{beam}}=35$ AMeV. Y_{X} is the yield of LCPs, Where $X=^{3}$He and ^{6}He, at mid-rapidity ($0<y^0<0.5$) or projectile rapidity region ($0.5<y^0<1.5$). The neutron-rich LCP are enhanced at mid-rapidity and it leads to a larger value of $R_{\mathrm{yield}}^{\mathrm{mid}}(^{6}\mathrm{He})$ which is close to the data for iso-MST case.

Table 1 The calculated results of $R\left(\frac{n}{p}\right)$, $R\left(\frac{t}{^{3}\mathrm{He}}\right)$ obtained for $^{124}\mathrm{Sn}+^{124}\mathrm{Sn}$ at $b=2$ fm, the results of $DR\left(\frac{n}{p}\right)$, $DR\left(\frac{t}{^{3}\mathrm{He}}\right)$ and α are obtained with an angular gate of $70^\circ \leqslant \theta_{\mathrm{c.m.}} \leqslant 110^\circ$ from two reaction systems $^{124}\mathrm{Sn}+^{124}\mathrm{Sn}$, $^{112}\mathrm{Sn}+^{112}\mathrm{Sn}$ at $b=2$ fm. The $R_{\mathrm{yield}}^{\mathrm{mid}}$ values are obtained for the reaction system $^{70}\mathrm{Zn}+^{70}\mathrm{Zn}$ at $b=4$ fm and $E_{\mathrm{beam}}=35$ AMeV

Observable*	MST	iso-MST
$R(\frac{\mathrm{n}}{\mathrm{p}})_{E_{\mathrm{k}}<40\ \mathrm{MeV}}(^{124}\mathrm{Sn})$	2.131 ± 0.005	2.302 ± 0.006
$R(\frac{\mathrm{n}}{\mathrm{p}})_{E_{\mathrm{k}}>40\ \mathrm{MeV}}(^{124}\mathrm{Sn})$	1.044 ± 0.011	1.041 ± 0.011
$DR(\frac{\mathrm{n}}{\mathrm{p}})_{E_{\mathrm{k}}<40\ \mathrm{MeV}}$	1.514 ± 0.005	1.641 ± 0.006
$DR(\frac{\mathrm{n}}{\mathrm{p}})_{E_{\mathrm{k}}>40\ \mathrm{MeV}}$	1.803 ± 0.029	1.852 ± 0.030
$R(\frac{\mathrm{t}}{^{3}\mathrm{He}})_{^{124}\mathrm{Sn}}$	3.031 ± 0.026	3.497 ± 0.028
$DR(\frac{\mathrm{t}}{^{3}\mathrm{He}})_{E_{\mathrm{k}}/A<40\ \mathrm{MeV}}$	1.57 ± 0.02	1.64 ± 0.02
$R_{\mathrm{yield}}^{\mathrm{mid}}(^{3}\mathrm{He})$	1.49 ± 0.01	1.49 ± 0.01
$R_{\mathrm{yield}}^{\mathrm{mid}}(^{6}\mathrm{He})$	1.78 ± 0.01	1.90 ± 0.01
Isoscaling parameter α	0.19	0.22

With larger R_0^{nn} and R_0^{np} values adopted in the iso-MST method, more neutron-rich isotopes are produced. This effect is further enhanced in the neutron-rich reaction system. Fig. 3 shows the isotope distributions of primary fragments with $Z=3\sim8$ predicted by the ImQMD05 calculations over the angle region, $70^\circ \leqslant \theta \leqslant 110^\circ$ for $^{124}\mathrm{Sn}+^{124}\mathrm{Sn}$ system. The solid circles are results obtained with the iso-MST method, and open circles are results obtained with the MST method.

http://www.npr.ac.cn

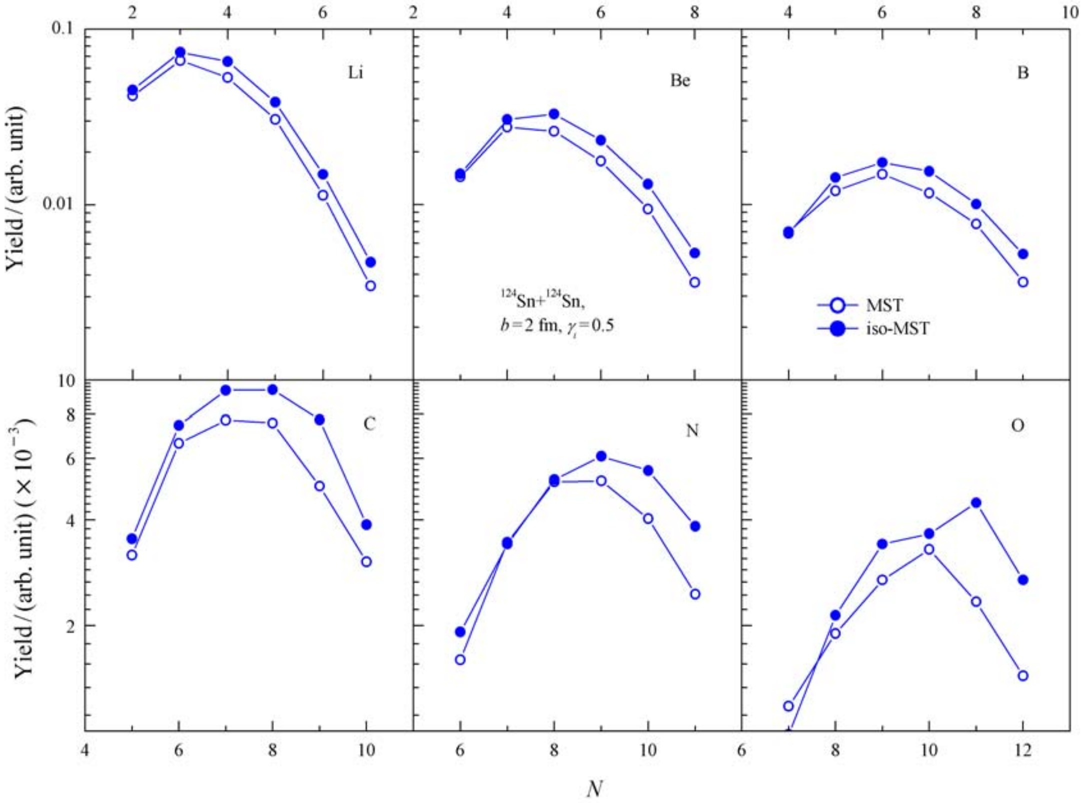

Fig. 3 (color online) Calculated primary isotope yields of Li, Be, B, C, N and O for ^{124}Sn + ^{124}Sn with an angular gate of $70^\circ \leqslant \theta_{\mathrm{c.m.}} \leqslant 110^\circ$ for $\gamma_i = 0.5$ at $b = 2$ fm.

The isoscaling relationship, which is constructed using isotope yields $Y_i(N, Z)$ with neutron number N and proton number Z from two different reaction systems denoted by the index i, obeys a simple relationship

$$R_{21}(N,Z) = \frac{Y_2(N,Z)}{Y_1(N,Z)} = C \cdot \exp(\alpha N + \beta Z)\,. \qquad (2)$$

Here, C is an overall normalized factor and α and β are isoscaling parameters. The isoscaling parameter α can be used to estimate the enhancement of neutron rich isotopes, and has been used as a probe to study the density dependence of symmetry energy[21, 30–32]. We analyze the isoscaling relationship with both cluster recognition methods for fragments with $Z = 3 \sim 8$. As in previous study[16], we find that the isoscaling relationship exists in non-equilibrium transport model. The best fit isoscaling parameters α are listed in Table 1. The isoscaling parameter α obtained with the MST is 0.19, and the α value obtained with the iso-MST case increases to 0.22 which is still less than the experimental value of $\alpha = 0.36 \pm 0.04$[31]. Sequential decays may modify the α values. However, results from current sequential decay calculations are model dependent[33–34]. Since the differences in α values are small, it will be difficult to determine the exact effects until more realistic sequential model calculations become available.

Finally, we examine the effects of isospin cluster recognition on the system equilibrium measured by the production of light particles. To characterize the degree of equilibrium reached in the collision system, the observable of $vartl = \frac{\sigma^2_{\mathrm{trans}}}{\sigma^2_{\mathrm{long}}}$ is often used in experimental and theoretical studies[18–19, 35]. Here, the σ^2_{tran} and σ^2_{long} are the variance of transverse and longitude rapidity distribution of fragment yields. When the reaction system reaches equilibrium, the value of $\frac{\sigma^2_{\mathrm{trans}}}{\sigma^2_{\mathrm{long}}}$ is close to 1. In Fig. 4, we plot the calculated results of longitudinal (a) and transverse (b) rapidity distribution for the Z-weighted yield ($Z = 1 \sim 6$) for ^{124}Sn + ^{124}Sn at $b = 2$ fm. The much wider longitudinal rapidity distributions suggest that the systems are far from equilibrium. More interestingly, the peaks in the longitudinal rapidity distribution (a) for $Z = 1 \sim 6$ particles obtained in the MST case diminishes in the iso-MST case. It suggests that a higher equilibrium degree is predicted in the iso-MST case. With $\gamma_i = 0.5$, the value of $vartl = \frac{\sigma^2_{\rm trans}}{\sigma^2_{\rm long}}$ obtained with the iso-MST case is 0.62, which is slightly larger than 0.58 for the MST case. Thus in addition to the isospin sensitive observables, the equilibrium or stopping power of the system also depends on the detailed description of cluster formation implemented in the transport models as well as on the mean field and the in-medium NN cross section.

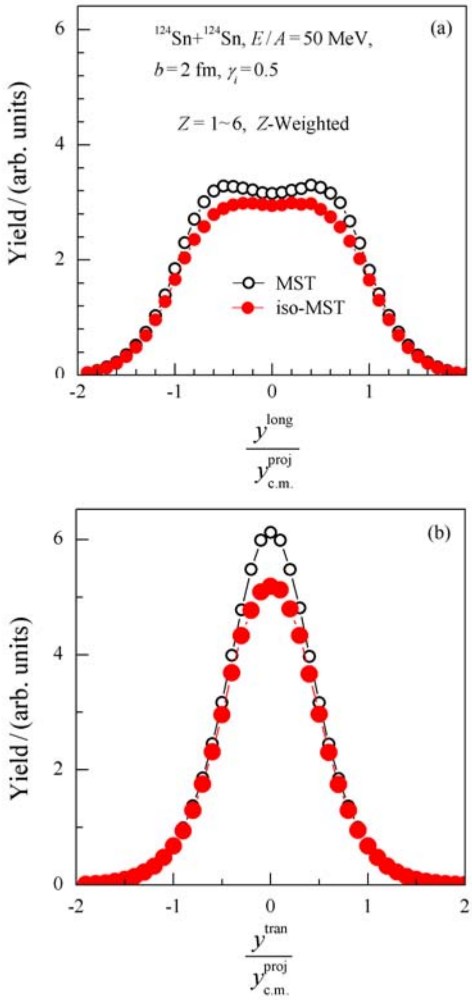

Fig. 4 (color online) The calculated results of longitudinal (a) and transverse (b) rapidity distribution for the Z-weighted yield ($Z = 1 \sim 6$) for ^{124}Sn+^{124}Sn at $b = 2$ fm.

3 Summary

In summary, we introduce a phenomenological isospin dependence in the description of cluster formation in transport models by adopting different R_0 values for p-p, nn and np, $R_0^{\rm pp} = 3$ fm and $R_0^{\rm nn} = R_0^{\rm np} = 6$ fm. Our results using the iso-MST show suppression of $Z = 1$ particles and enhancement of fragments, especially for heavier fragments with $Z \geqslant 12$. Furthermore, we find enhanced production of neutron-rich isotopes at mid-rapidity. Consequently, isospin sensitive observables, such as the double ratios, $DR\left(\frac{\rm t}{^3{\rm He}}\right)$, $R^{\rm mid}_{\rm yield}$ and isoscaling parameter α increase to larger values. The widths of the longitudinal and transverse rapidity distributions of $Z = 1 \sim 6$ particles also change. In all the observables that we examine, the effects introduced by the iso-MST algorithm are relatively small but in the direction of better agreement with data. However, we have not included sequential decays which may modify the magnitude of the effects. Nonetheless, the isospin dependence of the cluster recognition can be easily implemented and should be included in nuclear transport models.

References:

[1] BROWN B A. Phys Rev C, 1991, **43**: R1513.

[2] TSANG M B, ZHANG Yingxun, DANIELEWICZ P, *et al*. Phys Rev Lett, 2009, **102**: 122701.

[3] DANIELEWICZ P, LACEY R, LYNCH W G. Science, 2006, **298**: 1592.

[4] LI Bao-an, CHEN Lie-wen, KO Che-min. Phys Rep, 2008, **464**: 113.

[5] BONDORF J P, BOTVINA A S, ILJINOV A S, *et al*. Phys Rep, 1995, **257**: 133.

[6] GROSS D H E. Rep Prog Phys, 1990, **53**: 605.

[7] AICHELIN J. Phys Rep, 1991, **202**: 233.

[8] COLONNA M, FABBRI G. Nucl Phys A, 2004, **742**: 337.

[9] CHOMAZ P, COLONNA M, RANDRUP J. Phys Rep, 2004, **389**: 263.

[10] LE F A, AICHELIN J. Phys Rev Lett, 2008, **100**: 042701.

[11] DAS C B, GUPTA S D, LYNCH W G, *et al*. Phys Rep, 2005, **406**: 1.

[12] ZHANG Yingxun, COUPLAND D D S, DANIELEWICZ P, *et al*. Phys Rev C, 2012, **85**: 024602.

[13] COUPLAND D D S, LYNCH W G, TSANG M B, *et al*. Phys Rev C, 2011, **84**: 054603.

[14] LI Bao-an, CHEN Lie-wen. Phys Rev C, 2005, **72**: 064611.

[15] ZHANG Yingxun, DANIELEWICZ P, FAMIANO M, *et al*. Phys Lett B, 2008, **664**: 145.

[16] ONO A, DANIELEWICZ P, FREIDMAN W A, *et al*. Phys Rev C, 2003, **68**: 051601(R).

[17] ZHANG Yingxun, LI Zhuxia. Phys Rev C, 2005, **71**: 024604.

[18] ZHANG Yingxun, LI Zhuxia. Phys Rev C, 2006, **74**: 014602.

[19] ZHANG Yingxun, LI Zhuxia, DANIELEWICZ P. Phys Rev C, 2007, **75**: 034615.

[20] NEBAUER R, AICHELIN J (INDRA collaboration). Nucl Phys A, 1999, **658**: 67.
[21] LIU T X, VAN G M J, LIU X D, *et al*. Phys Rev C, 2004, **69**: 014603.
[22] RUSSOTO P, DE E, PAGANO A, *et al*. Phys Rev C, 2010, **81**: 064605.
[23] KOHLEY Z, MAY L W, WUENSCHEL S, *et al*. Phys Rev C, 2011, **83**: 044601.
[24] HUDAN S, CHBIHI A, FRANKLAND J D, *et al*. Phys Rev C 2003, **67**: 064613.
[25] DORSO C O, RANDRUP J. Phys Lett B, 1993, **301**: 328.
[26] PURI R K, AICHELIN J. J Comput Phys, 2000, **162**: 245.
[27] GOSSIAUX P B, PURI R K, HARTNACK C, *et al*. Nucl Phys A, 1997, **619**: 379.
[28] SUPRIYA G, RAJEEV K P. Phys Rev C, 2011, **83**: 047601.
[29] ZHANG Yingxum, LI Zhuxia, ZHOU Chengshuang, *et al*.Phys Rev C, 2012, **86**: 051602(R).
[30] XU H S, TSANG M B, LIU T X, *et al*. Phys Rev Lett, 2000, **85**: 716.
[31] TSANG M B, GELBKE C K, LIU X D, *et al*. Phys Rev C, 2001, **64**: 054615.
[32] SOUZA S R, TSANG M B, CARLSON B B, *et al*. Phys Rev C, 2009, **80**: 041602(R).
[33] TSANG M B, BOUGAULT R, CHARITY R, *et al*. Euro Phys Jour A, 2006, **30**: 129; Euro Phys Jour A, 2007, **32**: 243.
[34] COLONNA M, BARAN V, DI TORO M. *et al*. Phys Rev C, 2008, **78**: 064618.
[35] RESIDORF W, ANDRONIC A, GOBBI A, *et al*. (FOPI Collaboration). Phys Rev Lett, 2004, **92**: 232301.

同位旋依赖的碎块判断方法对重离子碰撞观测量的影响

张英逊[1, 1)]，李祝霞[1]，周承双[1, 2]，曾敏儿[3]

(1. 中国原子能科学研究院核物理研究所，北京 102413；
2. 广西师范大学物理系，广西 桂林 541004；
3. 密西根州立大学国家超导回旋加速器实验室，东兰辛 48824，美国)

摘要： 该工作提出了一个同位旋依赖碎块判断方法用以描述重离子碰撞过程中的碎块形成。利用该方法可以改善输运理论对于核子以及轻带电粒子产额的描写，其在计算中降低了发射核子产额、增加碎块(特别是丰中子碎块)的产额。对于丰中子轻带电粒子的增强主要出现在中心快度区。研究表明，该方法对于同位旋敏感的观测量，如 $\frac{\mathrm{n}}{\mathrm{p}}$，$\frac{\mathrm{t}}{^{3}\mathrm{He}}$，$R_{\mathrm{yield}}^{\mathrm{mid}}$ 和 isoscaling parameters 等，以及系统的平衡度的量度都会产生影响。

关键词： 同位旋依赖的碎块判断方法；同位旋敏感观测量；系统平衡度；重离子碰撞

收稿日期： 2012-10-21； **修改日期：** 2013-03-10

基金项目： 国家自然科学基金资助项目(11075215，10875031，11005022，11005155，11275052)；国家重点基础研究发展计划项目(973计划)(2013CB834404)；核能开发科研项目(科工二司)([2011]767)；美国国家自然科学基金资助项目(PHY-0606007)

1) E-mail: zhyx@ciae.ac.cn